This result qualitatively agrees with the fact that the cupferrate ligand is more symmetrical than the BPHA ligand.

As already mentioned, the quadrupole-coupling parameters measured in the two compounds $Na_4Hf(C_2O_4)_4 \cdot 3H_2O$ and $K_4Hf(C_2O_4)_4 \cdot 5H_2O$ have been interpreted by using the same approach.[11] The overall charge donated by the four oxalato ligands onto the valence orbitals of the metal in the Hf-$(C_2O_4)_4^{4-}$ anion was found to be roughly $-2e$. Such a value corresponds to an average ionicity of 50% for the hafnium-oxygen bonds, in agreement with the conclusions reached from infrared spectroscopy experiments.[36] This result must be connected with the significant dissymmetry observed in C–O distances within the $C_2O_4^{2-}$ ligand: whereas the four C–O bonds are equivalent in the free $C_2O_4^{2-}$ ion,[40] the two C–O bonds coordinated to the metal are lengthened, and the other two are shortened in the $Hf(C_2O_4)_4^{4-}$ (or isomorphous Zr-$(C_2O_4)_4^{4-}$) anion,[41,42] which is an indication for strong hafnium–oxygen interactions. According to our results, the charge donation would be noticeably lower in the three chelates Hf-$(NBPHA)_4$, Hf(cupferrate), and $Hf(T)_4$ than in the tetrakis-(oxalato)hafniate anion. Values between $-0.8e$ and $-1.2e$ for the total charge transferred onto the central ion suggest that the hafnium–oxygen interactions are greatly dominated by electrostatic forces in these neutral eight-coordinate d^0 complexes.

Registry No. $Hf(BPHA)_4$, 66673-11-8; Hf(cupferrate)$_4$, 38356-62-6; $Hf(T)_4$, 12367-98-5; $Hf(T)_4 \cdot DMF$, 61977-48-8; Hf(8-quin)$_4$, 21392-78-9.

References and Notes

(1) Orgel, L. E. *J. Inorg. Nucl. Chem.* **1960**, *14*, 136.
(2) Throughout this paper, the vertices and edges of the dodecahedron are labeled according to the nomenclature introduced by: Hoard, J. L.; Silverton, I. V. *Inorg. Chem.* **1963**, *2*, 235.
(3) Bonds, W. D.; Archer, R. D.; Hamilton, W. C. *Inorg. Chem.* **1971**, *10*, 1764.
(4) Bradley, D. C.; Hursthouse, M. B.; Rendall, I. F. *Chem. Commun.* **1970**, 368.
(5) Lewis, D. F.; Fay, R. C. *J. Chem. Soc., Chem. Commun.* **1974**, 1046.
(6) Tranqui, D.; Laugier, J.; Boyer, P.; Vulliet, P. *Acta Crystallogr., Sect. B* **1978**, *34*, 767.
(7) Steffen, W. L.; Fay, R. C. *Inorg. Chem.* **1978**, *17*, 2120.
(8) Parish, R. *Prog. Inorg. Chem.* **1972**, *15*, 101.
(9) Boyer, P.; Tissier, A.; Vargas, J. I.; Vulliet, P. *Chem. Phys. Lett.* **1972**, *14*, 601.
(10) Lowe, L. M.; Prestwich, W. V.; Zmora, H. *Can. J. Phys.* **1975**, *53*, 1327.
(11) Vulliet, P.; Baudry, A.; Boyer, P.; Tissier, A. *Chem. Phys. Lett.* **1978**, *55*, 297.
(12) Baudry, A.; Boyer, P.; Tissier, A. *Mol. Phys.* **1978**, *36*, 1037.
(13) Boussina, A.; Marques-Netto, A.; Abbe, J. Ch.; Haessler, A. *Radiochem. Radioanal. Lett.* **1976**, *24*, 43.
(14) Rasera, R. L.; Vincent, J. S. *Chem. Phys. Lett.* **1975**, *35*, 95.
(15) Ryan, D. E. *Can. J. Chem.* **1960**, *38*, 2488.
(16) Karlysheva, K. F.; Sheka, I. A. *Russ. J. Inorg. Chem. (Engl. Transl.)* **1962**, *7*, 666.
(17) Mark, W. *Acta Chem. Scand.* **1970**, *24*, 1398.
(18) Hutchinson, B.; Eversdyk, D.; Olbricht, S. *Spectrochim. Acta, Part A* **1974**, *30a*, 1605.
(19) Tissier, A. Thesis, Grenoble, 1977.
(20) Boyer, P.; Tissier, A.; Vargas, J. I. *Inorg. Nucl. Chem. Lett.* **1972**, *8*, 813.
(21) Tranqui, D.; Tissier, A.; Laugier, J.; Boyer, P. *Acta Crystallogr., Sect. B* **1977**, *33*, 392.
(22) Vinogradov, A. V.; Shpinel, V. S. *Russ. J. Inorg. Chem. (Engl. Transl.)* **1961**, *6*, 687.
(23) Frauenfelder, H.; Steffen, R. M. In "Alpha-, Beta-, and Gamma-Ray Spectroscopy"; Siegbahn, K., Ed.; North-Holland Publishing Co.: Amsterdam, 1965; Vol. 2, p 997.
(24) Shirley, D. A.; Haas, H. *Annu. Rev. Phys. Chem.* **1972**, *23*, 385.
(25) Yates, M. J. L. In "Alpha-, Beta-, and Gamma-Ray Spectroscopy"; Siegbahn, K., Ed.; North-Holland Publishing Co.: Amsterdam, 1965; Vol. 2, p 1691.
(26) Matthias, E.; Schneider, W.; Steffen, R. M. *Phys. Lett.* **1963**, *4*, 41.
(27) Muetterties, E. L.; Wright, C. M. *J. Am. Chem. Soc.* **1965**, *87*, 4706.
(28) La Rossa, R. A.; Brown, T. L. *J. Am. Chem. Soc.* **1974**, *96*, 2072.
(29) Brown, T. L. *Acc. Chem. Res.* **1974**, *7*, 408.
(30) Lucken, E. A. C. "Nuclear Quadrupole Coupling Constants", Academic Press: New York 1969; Chapter 5.
(31) Jeandey, Ch. Thesis, Grenoble, 1974.
(32) Desclaux, J. P., private communication.
(33) Feiock, F. D.; Johnson, W. R. *Phys. Rev.* **1969**, *187*, 39.
(34) Gupta, R. P.; Sen, S. K. *Phys. Rev. A* **1973**, *7*, 850.
(35) Sen, K. D.; Narasimhan, P. T. "Advances in Nuclear Quadrupole Resonance"; Smith, J. A. S., Ed.; Heyden: London, 1964; Vol. 1, p 277. According to these authors, the $(1 - \gamma_\infty)$ values for crystal cations are expected to be 30–50% higher than the values corresponding to free cations. Calculations performed with $(1 - \gamma_\infty) = 100$ for the Ta^{5+} ion lead to Δq values about 25% lower than those given in Table II.
(36) Johnson, F. A.; Larsen, E. M. *Inorg. Chem.* **1962**, *1*, 159.
(37) Gruen, E. C.; Plane, R. A. *Inorg. Chem.* **1967**, *6*, 1123.
(38) Duffey, G. H. *J. Chem. Phys.* **1950**, *18*, 1444.
(39) Due to the small value of α, the population of the $d_{x^2-y^2}$ orbital is weakly dependent on the charge transfer Δq given by the point-charge model. Consequently, it practically does not depend on the value taken for the $(1 - \gamma_\infty)$ antishielding factor.
(40) Jeffrey, G. A.; Parry, G. S. *J. Chem. Soc.* **1952**, 4864.
(41) Glen, G. L.; Silverton, J. V.; Hoard, J. L. *Inorg. Chem.* **1963**, *2*, 250.
(42) Tranqui, D.; Boyer, P.; Laugier, J.; Vulliet, P. *Acta Crystallogr., Sect. B* **1977**, *33*, 3126.

ENDOR Studies of [N,N'-Ethylenebis(salicylideniminato)]copper(II) in [N,N'-Ethylenebis(salicylideniminato)]nickel(II) Single Crystals

SHOUICHI KITA, MASAO HASHIMOTO, and MASAMOTO IWAIZUMI*

ENDOR spectra of [N,N'-ethylenebis(salicylideniminato)]copper(II) doped in [N,N'-ethylenebis(salicylideniminato)]nickel(II) single crystals are reported. Nitrogen hyperfine couplings, eight proton hyperfine couplings within the molecule, and five proton hyperfine couplings due to the neighboring molecules were determined. The quadrupole coupling tensor of the nitrogen nuclei was also obtained. From comparison with ligand hyperfine interactions for related copper(II) complexes, it is shown that the Cu–N bonds in [N,N'-ethylenebis(salicylideniminato)]copper(II) have a stronger covalency than that of copper(II) complexes with a trans N–Cu–N configuration, while Cu–O in the former has less covalency than in the latter complexes. The presence of a correlation between the orbital hybridization of the coordinating atoms and spin distribution in the ligands is also suggested. The electron populations on the nitrogen orbitals were evaluated from the quadrupole coupling tensor.

Introduction

For investigations of the nature of metal–ligand bonding in paramagnetic metal complexes, observation of superhyperfine interactions of ligand nuclei is useful. ENDOR is effective for the ligand hyperfine interaction and determination of the coupling constants with high accuracy.[1] In the present work,

[N,N'-ethylenebis(salicylideniminato)]copper(II), Cu(salen), in a single-crystal form doped into [N,N'-ethylenebis(salicylideniminato)]nickel(II), Ni(salen), has been examined by ENDOR spectroscopy. Though there have been several investigations of Schiff base complexes of copper(II) in single-crystal forms,[1e,f,2] we aimed to obtain more detailed information on

Table I. EPR Parameters

g_1	g_2	g_3	coupling constants of ^{63}Cu, cm^{-1}			dir cosines of g_1 and A_1			ref
			$10^4A_1/hc$	$10^4A_2/hc$	$10^4A_3/hc$	l_a	l_b	l_c	
2.192 ± 0.001	2.042 ± 0.002	2.042 ± 0.002	−201.1 ± 3.0	−29.7 ± 3.0	−29.7 ± 3.0	0.453	±0.088	±0.887	this work
2.192 ± 0.002	2.046 ± 0.004	2.049 ± 0.004	−201.0 ± 1.0	−30.7 ± 2.0	−32.7 ± 2.0	0.45	0	±0.89	2c

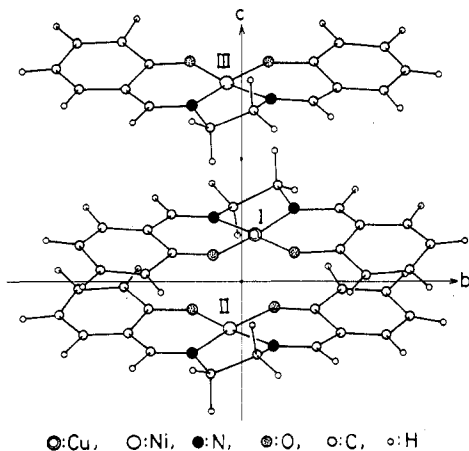**Figure 1.** Cu(salen).

O:Cu, O:Ni, ●:N, ⊚:O, o:C, ∘:H
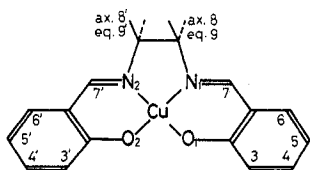
Figure 2. Crystal structure of copper doped Ni(salen).

the nature of metal–ligand bonding and on the effects of ligand variation on the bonding nature through observation of hyperfine interactions of the ligand nuclei.

Experimental Section

Cu(salen) and Ni(salen) were prepared according to the literature.[3] Single crystals of Ni(salen) containing approximately 0.5% Cu(salen) were grown from a saturated methanol solution. The Ni(salen) crystals are orthorhombic with space group *Pbca*, containing eight molecules per unit cell, and centrosymmetric dimers form the structure (Figure 2).[4] Though Cu(salen) is not isomorphous with Ni(salen), the substitutional site is treated as the same as that of Ni(salen) in this work. The ENDOR spectra were measured over a temperature range of 15–25 K with a Varian Model E1700 ENDOR spectrometer equipped with an Oxford Model ESR 9 cryostat. The angular dependence of the spectrum was obtained by measurements at 5–10° intervals by rotation of the crystal about three crystal axes. EPR spectra were measured with Hitachi Model 771 X-band and Model MES 400 K-band EPR spectrometers for determination of the g tensor.

Analysis of EPR and ENDOR Spectra

The spin Hamiltonian for the copper(II) complex is expressed as

$$\mathcal{H} = \underset{(a)}{\beta\tilde{H}\cdot g\cdot S} + \underset{(b)}{\tilde{S}\cdot A^{Cu}\cdot I^{Cu}} - \underset{(c)}{g_{Cu}\beta_n\tilde{H}\cdot I^{Cu}} + \underset{(d)}{\tilde{I}^{Cu}\cdot Q^{Cu}\cdot I^{Cu}} +$$

$$\sum_{i=1}^{2}(\underset{(e)}{\tilde{S}\cdot A^{N_i}I^{N_i}} - \underset{(f)}{g_N\beta_n\tilde{H}\cdot I^{N_i}} + \underset{(g)}{\tilde{I}^{N_i}\cdot Q^{N_i}\cdot I^{N_i}}) +$$

$$\sum_i(\underset{(h)}{\tilde{S}\cdot A^{H_i}I^{H_i}} - \underset{(i)}{g_H\beta_n\tilde{H}\cdot I^{H_i}}) \quad (1)$$

In this work, the EPR and ENDOR spectra are analyzed by eq 2–4, which are derived within the high-field approximation and by taking into account the conditions b ≫ c and d, e ≫ f and g, and h ≈ i or i > h under an arbitrary coordinate system.[5] In general, the condition b ≫ d, which allows use of the perturbation approach, may not necessarily hold near

the perpendicular orientation for planar copper(II) complexes. In the present case, however, the $Q_\perp/hc$ value at the perpendicular orientation was estimated to be -0.67×10^{-4} cm^{-1},[6] which indicates from comparison with the hyperfine coupling data (Table I) that the condition assumed here is valid as an approximation.

$$h\nu_{EPR} = g\beta H + K^{Cu}M_I^{Cu} +$$
$$\frac{1}{4g\beta H}\{[I^{Cu}(I^{Cu}+1) - (M_I^{Cu})^2]\,\mathrm{Tr}\,\tilde{A}^{Cu}\cdot A^{Cu} -$$
$$2(M_I^{Cu})^2(K^{Cu})^2 - [I^{Cu}(I^{Cu}+1) - 3(M_I^{Cu})^2]\tilde{h}\cdot\tilde{g}\cdot\tilde{A}^{Cu}\cdot A^{Cu}\cdot$$
$$\tilde{A}^{Cu}\cdot A^{Cu}\cdot g\cdot h/g^2(K^{Cu})^2\} + \sum_{i=1}^{2}K^{N_i}K^{N_i} + \sum_{i=7,7'}(K_+^{H_i} + K_-^{H_i})$$
$$(2)$$

$$h\nu_{ENDOR}^{N_i}(\pm,M_I \leftrightarrow M_{I-1}) = \frac{1}{2}K^{N_i} \mp g_N\beta_n H(\tilde{k}^{N_i}\cdot h) \pm$$
$$\frac{3}{2}(\tilde{k}^{N_i}\cdot Q^{N_i}\cdot k^{N_i}) + \frac{1}{4g\beta H}[|A_1^{N_i}|^2(2M_I^{N_i}-1) \mp A_2^{N_i} -$$
$$\frac{1}{2}A_3^{N_i}(2M_I^{N_i}-1) + (L^{Cu,N_i} - 2K^{Cu}K^{N_i})M_I^{Cu}] +$$
$$\frac{1}{K^{N_i}}[|Q_1^{N_i}|^2(24(M_I^{N_i})^2 - 24M_I^{N_i} + 1) -$$
$$\frac{1}{4}|Q_2^{N_i}|^2(6(M_I^{N_i})^2 - 6M_I^{N_i} - 1)] \quad (3)$$

$$h\nu_{ENDOR}^{H_i}(\pm) = K_\pm^{H_i} + \frac{\det A^{H_i}}{4g\beta H K_\pm^{H_i}}[\pm\frac{1}{2} - g_H\beta_n H(\tilde{h}\cdot\tilde{g}\cdot$$
$$(A^{H_i})^{-1}\cdot h)/g] \pm \frac{1}{4g\beta H}P^{Cu,H_i}M_I^{Cu} \quad (4)$$

where

$$g = (\tilde{h}\cdot\tilde{g}\cdot g\cdot h)^{1/2}$$

$$K^{Cu} = (\tilde{h}\cdot\tilde{g}\cdot\tilde{A}^{Cu}\cdot A^{Cu}\cdot g\cdot h)^{1/2}/g$$

$$K^{N_i} = (\tilde{h}\cdot\tilde{g}\cdot\tilde{A}^{N_i}\cdot A^{N_i}\cdot g\cdot h)^{1/2}/g$$

$$K_\pm^{H_i} = \{\tilde{h}\cdot[(\pm\frac{1}{2})(\tilde{g}\cdot\tilde{A}^{H_i}/g) \pm g_H\beta_n HE]\cdot[(\pm\frac{1}{2}) \times$$
$$(A^{H_i}\cdot g/g) \pm g_H\beta_n HE]\cdot h\}^{1/2}$$

$$k^{N_i} = A^{N_i}\cdot g\cdot h/gK^{N_i}$$

$$|A_1^{N_i}|^2 = (\tilde{k}^{N_i}\cdot A^{N_i}\cdot\tilde{A}^{N_i}\cdot k^{N_i}) - (K^{N_i})^2$$

$$A_2^{N_i} = \det A^{N_i}/K^{N_i}$$

$$A_3^{N_i} = \mathrm{Tr}\,\tilde{A}^{N_i}\cdot A^{N_i} - (\tilde{k}^{N_i}\cdot A^{N_i}\cdot\tilde{A}^{N_i}\cdot k^{N_i})$$

$$|Q_1^{N_i}|^2 = (\tilde{k}^{N_i}\cdot(Q^{N_i})^2\cdot k^{N_i}) - (\tilde{k}^{N_i}\cdot Q^{N_i}\cdot k^{N_i})^2$$

$$|Q_2^{N_i}|^2 = 2\,\mathrm{Tr}\,(Q^{N_i})^2 - 4(\tilde{k}^{N_i}\cdot(Q^{N_i})^2\cdot k^{N_i}) + (\tilde{k}^{N_i}\cdot Q^{N_i}\cdot k^{N_i})^2$$

$$gK^{Cu}K^{N_i}L^{Cu,N_i} = \tilde{h}\cdot\tilde{g}\cdot(\tilde{A}^{Cu}\cdot A^{Cu}\cdot\tilde{A}^{N_i}\cdot A^{N_i} +$$
$$\tilde{A}^{N_i}\cdot A^{N_i}\cdot\tilde{A}^{Cu}\cdot A^{Cu})\cdot g\cdot h$$

$$gK^{Cu}K_\pm^{H_i}P^{H_i,Cu} = \tilde{h}\cdot\tilde{g}\cdot(\tilde{A}^{Cu}\cdot A^{Cu}\cdot\tilde{g}^{-1}\cdot\tilde{K}_\pm^{H_i}A^{H_i} +$$
$$\tilde{g}^{-1}\cdot\tilde{K}_\pm^{H_i}\cdot A^{H_i}\cdot\tilde{A}^{Cu}\cdot A^{Cu})\cdot g\cdot h - 2(K^{Cu})^2(\tilde{h}\cdot\tilde{K}_\pm^{H_i}A^{H_i}\cdot g\cdot h)$$

The second term in eq 2 and the terms from the fourth to the last in eq 3 and from the second to the last in eq 4 are the second-order contribution, respectively, and the ± sign indicates $M_S = \pm\frac{1}{2}$ throughout the equations.

The second term in eq 4 is on the order of 10^{-3} MHz for the case $g\beta H = 9$ GHz and a proton hyperfine coupling constant of 10 MHz, and it is neglected in the present work.

Table II. Hyperfine Coupling Parameters of Protons

| posn	coupling constants, MHz				dir cosines of A_1			dir cosines of Cu–H (X-ray data)			dist of Cu–H, Å		rms, MHz
	A_1/h	A_2/h	A_3/h	a_{iso}/h	l_a	l_b	l_c	l_a	l_b	l_c	ENDOR	X-ray	
7	22.80	19.38	18.43	20.22	0.372	0.890	−0.264	0.465	0.817	−0.341	3.97	3.78	0.10
7'	23.62	19.45	18.64	20.57	0.397	−0.877	−0.272	0.489	−0.827	−0.279	3.76	3.73	0.10
3	1.77	−1.34	−1.87	−0.48	−0.639	0.614	0.464	−0.640	0.655	0.402	4.16	4.43	0.05
3'	1.84	−1.26	−1.39	−0.27	−0.648	−0.633	0.423	−0.637	−0.650	0.414	4.25	4.42	0.05
8	5.13	−0.90	−3.47	0.76	0.582	0.002	−0.813	0.655	0.171	−0.736	3.37	3.36	0.03
9	8.74	4.29	3.56	5.53	0.890	0.316	−0.330	0.873	0.340	−0.349	3.71	3.69	0.03
8'	5.54	−1.41	−1.43	0.90	0.996	−0.055	0.075	0.980	−0.190	0.024	3.30	3.19	0.03
9'	9.57	5.32	4.40	6.43	0.833	−0.304	−0.463	0.840	−0.364	−0.402	3.74	3.67	0.03
8'(II)	4.38	−1.21	−2.81	0.12	−0.541	0.023	0.841	−0.541	−0.008	0.841	3.39	3.29	0.05
8(III)	7.21	−2.77	−3.92	0.17	−0.344	0.405	0.847	−0.331	−0.457	−0.825	2.87	2.63	0.05
9(III)	2.87	−0.98	−1.89	0.00	−0.489	0.124	−0.863	−0.491	−0.042	−0.870	3.90	3.85	0.05
9(IV)	2.81	−1.00	−1.51	0.10	−0.977	0.201	0.079	−0.941	0.320	−0.099	3.98	3.92	0.05
9'(IV)	2.52	−0.94	−1.85	−0.09	−0.958	−0.285	0.035	−0.935	−0.326	0.141	3.98	4.09	0.05
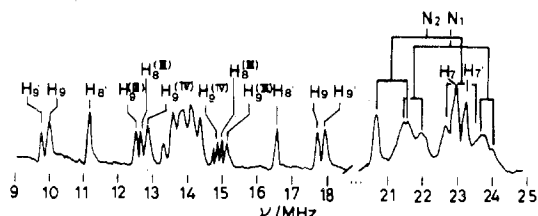
Figure 3. ENDOR spectrum obtained with the magnetic field parallel to the *a* axis. The signals due to the extra molecular protons are indicated by the symbol with a number in parentheses. The number IV is for the molecule situated behind I in Figure 2.
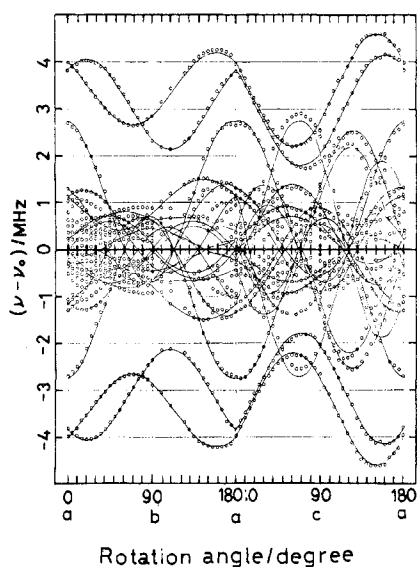

Figure 5. Angular dependence of the proton ENDOR signals which appeared in the 23-MHz region.

Figure 4. Angular dependence of the proton ENDOR signals which appeared near the free proton frequency region.
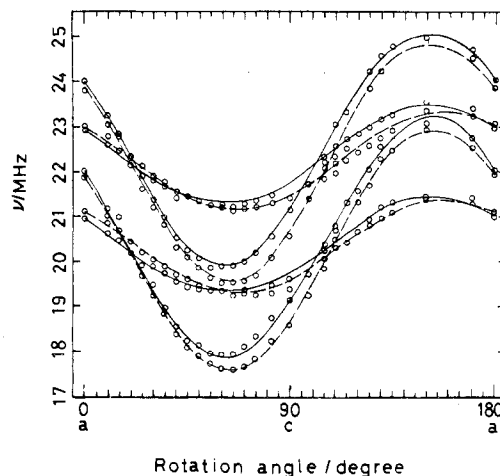
Figure 6. Angular dependence of the nitrogen ENDOR signals for the *b*-axis rotation.

The other second-order terms have some appreciable contribution to the ENDOR frequencies. Among them the effect of the cross terms between A^{Cu} and A^{N_i} and between A^{Cu} and A^{H_i} can be distinguished from the others because the nitrogen and proton ENDOR lines observed by applying the magnetic field on a $+M_I{}^{Cu}$ line shift at the same magnitude as but in the opposite direction to that observed by applying the field on a $-M_I{}^{Cu}$ line, so that the mean ENDOR frequencies with $+M_I{}^{Cu}$ and $-M_I{}^{Cu}$ do not change by the effect. The contribution of these cross terms is appreciable when the nuclei have large anisotropic hyperfine interaction.

The **g** tensor needed for the ENDOR analysis was obtained from the EPR analysis in the present work. The obtained tensor was in agreement with that reported by Scullane and Allen[2c] within experimental error. The EPR parameters are summarized in Table I.
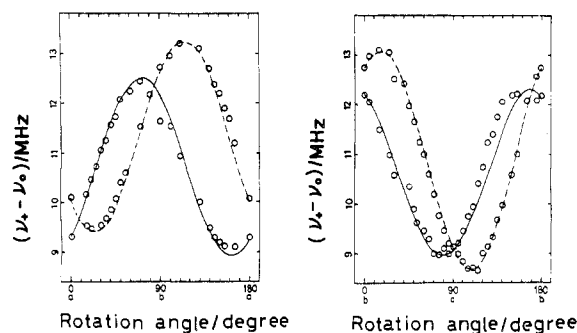
Results and Discussion

Figure 3 shows a typical ENDOR spectrum observed in this work. The proton signals are observed at 9–19 MHz and about the 23-MHz region. The signals from the nitrogen nuclei at two magnetically different sites are observed at 20–24 MHz as eight lines. The angular dependence of the proton and nitrogen ENDOR signals are given in Figures 4–7. The hyperfine and quadrupole coupling parameters were obtained by a least-squares procedure. For larger line widths and mutual overlap of the nitrogen ENDOR lines, accuracy of the ENDOR parameters for the nitrogen nuclei could not be improved as for the protons in the analysis.

Proton Coupling Constants. The eight proton coupling constants within the molecule and the five proton coupling constants due to the neighbor molecules were determined as listed in Table II. The pseudocontact interactions are estimated to be less than 0.05 MHz and hence they were neglected

Table III. Hyperfine Coupling Parameters of Nitrogen Nuclei

		principal values, MHz	dir cosines			dir cosines of N–Cu (X-ray data)			rms, MHz
			l_a	l_b	l_c	l_a	l_b	l_c	
N_1	$A_{\alpha\alpha}{}^N/h$	50.2	0.723	0.571	−0.390	0.637	0.644	−0.393	0.21
	$A_{\beta\beta}{}^N/h$	37.2	0.522	−0.820	−0.233				
	$A_{\gamma\gamma}{}^N/h$	39.1	0.453	0.035	0.891				
N_2	$A_{\alpha\alpha}{}^N/h$	50.9	0.715	−0.614	−0.334	0.674	−0.681	−0.288	0.27
	$A_{\beta\beta}{}^N/h$	37.0	0.551	0.789	−0.272				
	$A_{\gamma\gamma}{}^N/h$	38.8	0.431	0.011	0.902				

Table IV. Quadrupole Coupling Parameters of Nitrogen Nuclei

		principal values,[a] MHz	dir cosines			coupling parameters, MHz
			l_a	l_b	l_c	
N_1	$Q_{\alpha''\alpha''}{}^N/h$	−1.04	0.730	0.587	−0.349	$e^2Qq/h = -2.1, \eta = 0.32$
	$Q_{\beta''\beta''}{}^N/h$	0.69	0.634	−0.773	0.026	
	$Q_{\gamma''\gamma''}{}^N/h$	0.36	0.254	0.240	0.937	
N_2	$Q_{\alpha''\alpha''}{}^N/h$	−1.21	0.624	−0.694	−0.359	
	$Q_{\beta''\beta''}{}^N/h$	0.68	0.543	0.716	−0.439	$e^2Qq/h = -2.4, \eta = 0.13$
	$Q_{\gamma''\gamma''}{}^N/h$	0.52	0.562	0.079	0.824	

[a] Estimated error is ±0.05 MHz.

in the factoring of the hyperfine coupling data in Table II. The assignment of the observed proton hyperfine couplings were made by comparison of their direction cosines with those of Cu–H vector calculated from the crystallographic data,[4] since the unpaired electron is mainly located on the copper(II) ion and the principal axes of the proton hyperfine couplings are considered to orient to the Cu–H direction. The agreements between the direction cosines of the principal axes of the hyperfine interactions and the crystallographic Cu–H vectors are satisfactory. The Cu–H distances calculated from the anisotropic dipolar couplings on the basis of the point-dipole approximation and by assuming the unpaired electron density of 0.8 on copper also agree with those calculated from the crystallographic data.

As Table II shows, the protons at 7 and 7′ positions have large positive isotropic hyperfine coupling constants. For the corresponding protons in [N,N'-ethylenebis(o-amino-benzylideniminato)]copper(II), Cu(amben), and bis(N-methylsalicylaldiminato)copper(II), Cu(N-mesal)$_2$, slightly smaller isotropic hyperfine coupling constants have been reported,[2b,d] while the isotropic coupling constant reported for the corresponding protons in bis(salicylaldoximato)copper(II), Cu(saloxm)$_2$,[1e] was nearly half of those in Cu(salen) observed here (Table V). It is also notable that the isotropic hyperfine coupling constants of the protons at 3 and 3′ in Cu(salen) are negative but their absolute values are smaller than that observed for the corresponding protons, −0.59 MHz, in Cu(saloxm)$_2$.[1e,f] On the other hand, the isotropic coupling constants of the equatorial protons in the ethylene bridge are larger than those for axial ones. Such variety of the isotropic couplings of intramolecular protons shows structure sensitivity of the spin distribution in the ligand. The negative sign of the isotropic coupling constants for the protons at the 3 and 3′ positions may be explained by the spin-polarization effect. Figure 8 shows that the spin will be positively polarized at the 7, 7′, 8, 8′, 9 and 9′ positions and negatively polarized at the 3 and 3′ positions, in accord with the experimental observation.

For intermolecular protons the couplings are mostly anisotropic. The 8(III) proton has a large anisotropic coupling as it is closely situated to the copper(II) ion, but the isotropic contribution is negligible, a fact to be expected for intermolecular interaction.

Nitrogen Coupling Constants and Spin Populations on Nitrogen Orbitals. As Tables III and IV show, the hyperfine and quadrupole coupling tensors slightly deviate from axial symmetry and the unique axes are directed to the copper ion within 7°. In the nitrogen hyperfine interaction, the dipolar couplings
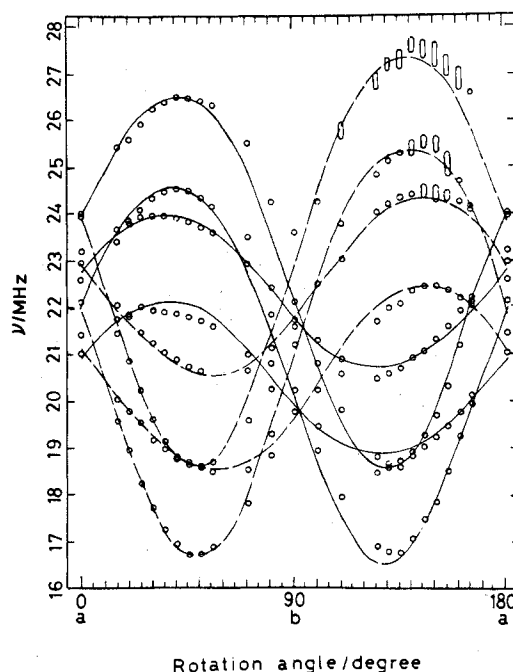

Figure 7. Angular dependence of the nitrogen ENDOR signals for the c-axis rotation.
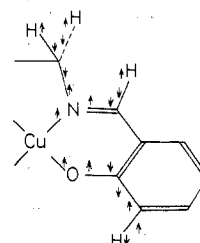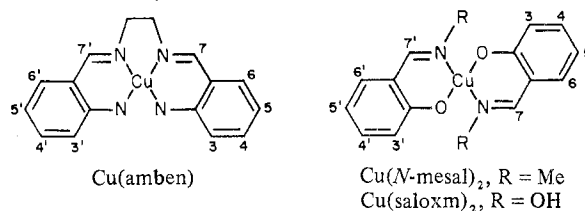

Figure 8. Spin polarization in the Cu(salen) ligand.

with the delocalized unpaired electron on nitrogen have some appreciable contribution and the hyperfine principal values are expressed as

$$A_{\alpha\alpha}{}^N = A_s{}^N + A_{p\alpha\alpha}{}^N + A_{d\alpha\alpha}{}^N$$

$$A_{\beta\beta}{}^N = A_s{}^N + A_{p\beta\beta}{}^N + A_{d\beta\beta}{}^N \tag{5}$$

$$A_{\gamma\gamma}{}^N = A_s{}^N + A_{p\gamma\gamma}{}^N + A_{d\gamma\gamma}{}^N$$

where $A_s{}^N$ is an isotropic coupling and $A_{pii}{}^N$ and $A_{dii}{}^N$ are

Table V. Unpaired Electron Populations on the Nitrogen Orbitals

Cu(amben)

Cu(N-mesal)$_2$, R = Me
Cu(saloxm)$_2$, R = OH

| | | | | | f_s/f_α | | | |
complex	f_s	f_α	f_β	f_γ	ENDOR or EPR	cryst data	$f_s + f_\alpha$	$a_{iso}(H_7)$
Cu(salen)[a]	0.027	0.071	0.0[c]	0.015	0.38	0.41	0.098	20.22
	0.027	0.077	0.0[c]	0.015	0.35	0.31	0.104	20.57
Cu(amben)	0.031[b]	0.078[b]			0.40		0.109	17[a]
Cu(N-mesal)[b]	0.025	0.06			0.42		0.085	14
Cu(saloxm)[a]	0.031	0.051	0.0[c]	0.012	0.61	0.66	0.082	10.17

[a] ENDOR data. $a_{iso}(H_7)$ for Cu(amben) was estimated from the powder ENDOR in this work. [b] EPR data. [c] f_β is assumed to be zero in the calculations of the unpaired electron populations.
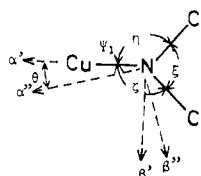

Figure 9. Coordinates of the nitrogen orbitals and quadrupole interaction tensor.

dipolar couplings with the unpaired electron on nitrogen and copper(II), respectively. The principal axis directed nearly to the copper(II) ion is defined as α and that normal to the molecular plane is γ. Each term in eq 5 has the forms

$$A_s^N = A_s f_s = \frac{8\pi}{3}h^{-1}g_N\beta_n g\beta|\psi_{2s}(0)|^2 f_s$$

$$A_{p\alpha\alpha}^N = A_p(2f_\alpha - f_\beta - f_\gamma)$$

$$A_{p\beta\beta}^N = A_p(2f_\beta - f_\gamma - f_\alpha) \tag{6}$$

$$A_{p\gamma\gamma}^N = A_p(2f_\gamma - f_\alpha - f_\beta)$$

$$A_p = \frac{2}{5}h^{-1}g_N\beta_n g\beta\langle 1/r^3\rangle_{2p}$$

$$A_{d\alpha\alpha}^N = \left(\frac{2P}{a^3}\right)\left[1 + \frac{6}{7}\left(\frac{\langle r^2\rangle}{a^2}\right)\right]f_d$$

$$A_{d\beta\beta}^N = -\left(\frac{P}{a^3}\right)\left[1 + \frac{3}{7}\left(\frac{\langle r^2\rangle}{a^2}\right)\right]f_d \tag{7}$$

$$A_{d\gamma\gamma}^N = -\left(\frac{P}{a^3}\right)\left[1 + \frac{9}{7}\left(\frac{\langle r^2\rangle}{a^2}\right)\right]f_d$$

$$P = g_N\beta_n g\beta h^{-1}$$

In the equations, f_s denotes the population of the unpaired electron on the 2s nitrogen orbital, f_α, f_β, and f_γ denote the populations on the 2p nitrogen orbitals, and f_d is the population on the 3d copper orbital. The pseudocontact interaction of the nitrogen nuclei was evaluated to be about −0.01 MHz and it was ignored in the analysis for Table IV.

Assuming an unpaired electron population of 0.8 on the copper(II) ion, we calculated the $A_{d\alpha\alpha}^N$, $A_{d\beta\beta}^N$, and $A_{d\gamma\gamma}^N$ values by eq 7. From the remaining terms in eq 5 and by use of the values of $A_s = 1540$ MHz and $A_p = 48$ MHz,[7] the unpaired electron populations on the nitrogen orbitals were evaluated. The results are listed in Table V together with the spin populations for Cu(saloxm)$_2$, Cu(N-mesal)$_2$, and Cu(am-

ben) obtained in a similar way from their hyperfine coupling tensors.[1e,2b,d]

Table V shows that the f_s, f_α, and their ratios vary in the series of the copper(II) complexes. The s/p ratios of the nitrogen lone pair orbitals expected from the molecular geometries were calculated for the two complexes of Cu(salen) and Cu(saloxm)$_2$ through the orbital expressions

$$\Psi_1 = A\psi_s + B\psi_{p\alpha}$$

$$\Psi_2 = C\psi_s + D(\psi_{p\alpha'}\cos\zeta - \psi_{p\beta'}\sin\zeta) \tag{8}$$

$$\Psi_3 = E\psi_s + F(\psi_{p\alpha'}\cos\eta + \psi_{p\beta'}\sin\eta) \qquad \Psi_4 = \psi_{p\gamma'}$$

where

$$A = \left(\frac{\cos\eta\cos\zeta}{\cos\eta\cos\zeta - \cos\xi}\right)^{1/2} \qquad B = (1 - A^2)^{1/2}$$

$$C = \left(\frac{\cos\xi\cos\zeta}{\cos\xi\cos\zeta - \cos\eta}\right)^{1/2} \qquad D = (1 - C^2)^{1/2}$$

$$E = \left(\frac{\cos\xi\cos\eta}{\cos\xi\cos\eta - \cos\zeta}\right)^{1/2} \qquad F = (1 - E^2)^{1/2}$$

α', β', γ', ζ, η, and ξ are defined on the basis of the molecular geometry as is shown in Figure 9. The s/p ratio of the orbital Ψ_1 is, hence, given by
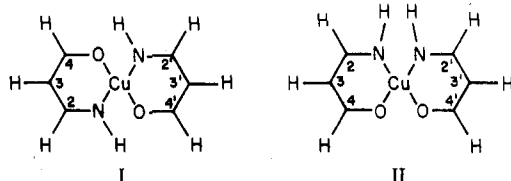
$$s/p = -\cos\eta\cos\zeta/\cos\xi \tag{9}$$

The geometries of the copper(II) complexes were taken from the crystallographic data of the copper(II) complex crystals;[7] because of a lack of X-ray data, the calculation was not made for Cu(amben) and Cu(N-mesal)$_2$. Clearly the calculated s/p ratios agree well with the s/p ratios evaluated from the nitrogen hyperfine coupling tensors.

Table V shows that the isotropic proton hyperfine coupling constants at the 7 and 7′ positions correlate with the unpaired electron population on the nitrogen atom; i.e., the larger f_α is, the larger $a_{iso}(H_7)$ is; the smaller f_s/f_α is, the larger $a_{iso}(H_7)$ is; and the larger $f_s + f_\alpha$ or $f_s + f_\alpha + f_\gamma$ is, the larger $a_{iso}(H_7)$ is. It is interesting that this correlation of the isotropic coupling constants of the 7 and 7′ protons is better with the unpaired electron density on $\psi_{p\alpha}$ or the s/p ratio of the nitrogen orbital than with the total unpaired electron density on the nitrogen or its in-plane orbital.

Correlation between the Spin Distribution and N–Cu–N Configuration. It seems valuable to note that the hyperfine interactions of the ligand nuclei reflect well changes in the metal–ligand interaction by going from trans to cis configu-

Table VI. Spin Densities by MO Calculation

	N^a	O^a	H(2,2')	H(4,4')
I	0.0356	0.0586	0.0129	0.0148
II	0.0455	0.0510	0.0151	0.0130

^{a} Total spin densities of in-plane orbitals.

ration in the N–Cu–N arrangement of the complexes. It was mentioned above that the isotropic proton hyperfine coupling constants at the 7 and 7' positions increase in the order Cu-(saloxm)$_2$ < Cu(*N*-mesal)$_2$ < Cu(amben) < Cu(salen) (Table V), while the protons at the 3 and 3' positions of Cu(salen) have smaller isotropic hyperfine coupling constants (in absolute value) than that observed for the corresponding protons of Cu(saloxm)$_2$. It is also seen from Table V that the spin densities on the nitrogen $\psi_{p\alpha}$ or Ψ_1 orbital increase in the order Cu(saloxm)$_2$ < Cu(*N*-mesal)$_2$ < Cu(amben), Cu(salen). These results indicate that the unpaired electron delocalization on nitrogen becomes larger while that on oxygen becomes smaller when the N–Cu–N arrangement takes a cis configuration. These changes in the unpaired electron densities on the coordinating atoms cause the changes in the spin distribution in the ligands, and at the nitrogen-side protons in the complexes with a cis N–Cu–N configuration more spin densities are distributed than those in the complexes with a trans N–Cu–N configuration, while at the oxygen-side protons in the complexes with a cis N–Cu–N configuration less spin densities are polarized than those in a trans configuration as was observed by the changes in the hyperfine coupling constants of the 3, 3' and 7, 7' protons.

Such variation in the spin distribution with the arrangement of the coordinating atoms can be also shown by a model calculation using the MO method based on an INDO approximation.[9] As Table VI shows, apparently the spin densities on the nitrogen and on the 2 and 2' protons increase while those on the oxygen and 4 and 4' protons decrease when the takes on a cis configuration.

These facts indicate that an appreciable mixing of $3d_{z^2}$ and 4s orbitals with the d_{xy} unpaired electron orbital occurs in the copper(II) complexes with the trans configuration of N–Cu–N, so that the electron orbital lobe at the nitrogen side decreases while it increases at the oxygen side, resulting in a decrease of overlap between the copper and nitrogen orbitals and an increase of overlap between the copper and oxygen orbitals. Such an orbital mixing will not effectively occur in the complexes with the cis N–Cu–N configuration because the mixing requires a 4p orbital.

It was pointed out above that there may be a correlation between the s/p ratio of the nitrogen orbital and the proton hyperfine coupling constants at 7-position. These facts seem to imply that there may be also some correlation between the N–Cu–N configuration and the hybridization of the coordinating nitrogen and oxygen atoms. However, since other effects, such as the presence of the ethylene bridge, will probably affect the molecular geometry and hence the orbital hybridization, it is impossible to prove the presence of the correlation at present.

Quadrupole Coupling Tensor. The quadrupole coupling Hamiltonian $\tilde{\mathbf{I}}\cdot\mathbf{Q}\cdot\mathbf{I}$ is expressed as

$$\mathcal{H}_Q = \frac{e^2qQ}{4I(2I-1)}[3I_z^2 - I(I+1)] + \frac{1}{2}\eta(I_+^2 + I_-^2) \quad (10)$$

and hence the quadrupole coupling tensor for nitrogen ($I = 1$) in the field gradient V can be written as

$$\mathcal{H}_Q = \begin{vmatrix} -\frac{1}{4}e^2qQ(1+\eta) & 0 & 0 \\ 0 & -\frac{1}{4}e^2qQ(1-\eta) & 0 \\ 0 & 0 & \frac{1}{2}e^2qQ \end{vmatrix} \quad (11)$$

where $eq = V_{\alpha''\alpha''}$ and $\eta = |V_{\beta''\beta''} - V_{\gamma''\gamma''}|/V_{\alpha''\alpha''}$. Thus, from the experimentally obtained quadrupole coupling tensor, the quadrupole coupling constant e^2qQ/h and asymmetry parameter η could be obtained to be −2.1 MHz and 0.32 for N_1 and −2.4 MHz and 0.13 for N_2, respectively. It is notable that these quadrupole coupling constants are appreciably smaller than the ordinary values, −4 to −5 MHz in the absolute values, for noncoordinating C—N=C nitrogen.

The obtained quadrupole coupling constants, e^2Qq_{ii}, can be correlated with the electron occupancy of each nitrogen hybrid orbital. Following Hsieh et al.,[10] we use eq 12 and 13 under

$$e^2Qq_{\alpha'\alpha'}/e^2Qq_0 = B^2l + (\cos^2 \zeta - \tfrac{1}{2}\sin^2 \zeta)D^2\sigma_2 + (\cos^2 \eta - \tfrac{1}{2}\sin^2 \eta)F^2\sigma_3 - \tfrac{1}{2}\pi \quad (12a)$$

$$e^2Qq_{\beta'\beta'}/e^2Qq_0 = -\tfrac{1}{2}B^2l + (\sin^2 \zeta - \tfrac{1}{2}\cos^2 \zeta)D^2\sigma_2 + (\sin^2 \eta - \tfrac{1}{2}\cos^2 \eta)F^2\sigma_3 - \tfrac{1}{2}\pi \quad (12b)$$

$$e^2Qq_{\gamma'\gamma'}/e^2Qq_0 = -\tfrac{1}{2}(B^2l + D^2\sigma_2 + F^2\sigma_3) + \pi \quad (12c)$$

$$e^2Qq_{\alpha'\beta'}/e^2Qq_0 = \tfrac{3}{4}(\sin 2\eta F^2\sigma_3 - \sin 2\zeta D^2\sigma_2) \quad (12d)$$

$$e^2Qq_{\alpha'\alpha'} = e^2Qq_{\alpha''\alpha''} \cos^2 \theta + e^2Qq_{\beta''\beta''} \sin^2 \theta \quad (13a)$$

$$e^2Qq_{\beta'\beta'} = e^2Qq_{\alpha''\alpha''} \sin^2 \theta + e^2Qq_{\beta''\beta''} \cos^2 \theta \quad (13b)$$

$$e^2Qq_{\gamma'\gamma'} = e^2Qq_{\gamma''\gamma''} \quad (13c)$$

$$e^2Qq_{\alpha'\beta'} = \tfrac{1}{2}(e^2Qq_{\alpha''\alpha''} - e^2Qq_{\beta''\beta''}) \sin 2\theta \quad (13d)$$

the coordinate systems of Figure 9, where α', β', and γ' are the coordinate axes based on the molecular geometry and α'', β'', and γ'' are the principal axes of the quadrupole interaction. In the equations, B, D, and F are given by eq 8 and they are obtained from the crystallographic data; l, σ_2, σ_3, and π are the respective occupancies of the orbitals Ψ_1, Ψ_2, Ψ_3, and Ψ_4 in eq 8. The quantity e^2Qq_0 is the quadrupole coupling arising from a single 2p electron on nitrogen and a value of 8–10 MHz is assigned. Because nitrogen is more electronegative than carbon, we assume here that $\sigma_2 = \sigma_3 = 1.20$. Thus l, π, and the net charge on nitrogen are calculated by these equations to be 1.62, 1.27, and −0.29 for N_1 and 1.61, 1.23, and −0.24 for N_2, respectively. Apparently the values of l are appreciably reduced from 2.0, which is a value for noncoordinating nitrogen, a fact reflecting the donation of electrons from the Ψ_1 orbital to the copper orbitals. The difference in the value of π between coordinating and free nitrogen is small.

Appendix

In this Appendix we consider ENDOR signal frequencies for protons and nitrogen nuclei of the ligand in metal complexes of $S = \frac{1}{2}$. The spin Hamiltonian is expressed as

$$\mathcal{H} = \beta\tilde{\mathbf{H}}\cdot\mathbf{g}\cdot\mathbf{S} + \sum_j \tilde{\mathbf{I}}^{(j)}\cdot\mathbf{A}^{(j)}\cdot\mathbf{S} - g_n^{(j)}\beta_n\tilde{\mathbf{H}}\cdot\mathbf{I}^{(j)} + \tilde{\mathbf{I}}^{(j)}\cdot\mathbf{Q}^{(j)}\cdot\mathbf{I}^{(j)}$$

$$(A1)$$

In eq A1, j refers to the metal ion, nitrogen nuclei, and protons but for protons the last term is dropped off. In the following,

m, n, and h are assigned to j for the metal ion, nitrogen nuclei, and protons, respectively. Assuming the same condition as in eq 1, one derives the following zeroth-, first-, and second-order energy expressions:[5,11,12]

$$E^{(0)}(M_S, M_I^{(m)}, M_I^{(n)}, M_I^{(h)}) = g\beta H M_S \quad (A2)$$

$$E^{(1)}(M_S, M_I^{(m)}, M_I^{(n)}, M_I^{(h)}) = A^{(m)} + \sum_n A^{(n)} + \sum_h K^{(h)}(M_S) M_I \quad (A3)$$

$$E^{(2)}(M_S, M_I^{(m)}, M_I^{(n)}, M_I^{(h)}) = B^{(m)} + \sum_n B^{(n)} + \sum_h C^{(c)} + \frac{1}{2g\beta H}[\sum_n (L^{(m,n)} - 2K^{(m)}K^{(n)})M_S M_I^{(m)} M_I^{(n)} + \sum_h P^{(m,h)} M_S M_I^{(m)} M_I^{(h)}] \quad (A4)$$

where

$$A^{(j)} = K^{(j)} M_S M_I^{(j)} - \tfrac{1}{2}(\tilde{k}^{(j)} \cdot Q^{(j)} \cdot k^{(j)}) \times [I^{(j)}(I^{(j)} + 1) + 3(M_I^{(j)})^2] - g_n^{(j)}\beta_n H(\tilde{k}^{(j)} \cdot h)M_I^{(j)}$$
$$j = m \text{ or } n$$

$$B^{(j)} = \frac{1}{2g\beta H}\{|A_1^{(j)}|^2 M_S(M_I^{(j)})^2 - A_2^{(j)}[S(S+1) - (M_S)^2]M_I^{(j)} + \tfrac{1}{2}A_3^{(j)} M_S[I^{(j)}(I^{(j)}+1) - (M_I^{(j)})^2]\} - \frac{1}{2K^{(j)} M_S}\{|Q_1^{(j)}|^2 M_I^{(j)}[4I^{(j)}(I^{(j)}+1) - 8(M_I^{(j)})^2 - 1] - \tfrac{1}{4}|Q_2^{(j)}|^2 M_I^{(j)}[2I^{(j)}(I^{(j)}+1) - 2(M^{(j)})^2 - 1]\}$$
$$j = m \text{ or } n$$

$$C^{(h)} = \frac{1}{2g\beta H}\{|A_1^{(h)}|^2 M_S(M_I^{(h)})^2 - A_2^{(h)}[S(S+1) - (M_S)^2]M_I^{(h)} + \tfrac{1}{2}A_3^{(h)} M_S[I^{(h)}(I^{(h)}+1) - (M_I^{(h)})^2]\}$$

$$g^2 = \tilde{h} \cdot \tilde{g} \cdot g \cdot h$$

$$g^2(K^{(j)})^2 = \tilde{h} \cdot \tilde{g} \cdot \tilde{A}^{(j)} \cdot A^{(j)} \cdot g \cdot h$$
$$j = m \text{ or } n$$

$$(K^{(h)}(M_S))^2 = \tilde{h} \cdot [(\tilde{g} \cdot \tilde{A}^{(h)}/g)M_S - g_H \beta_n H E] \times [(A^{(h)} \cdot g/g)M_S - g_H \beta_n H E] \cdot h$$

$$k^{(j)} = A^{(j)} \cdot g \cdot h / g K^{(j)}$$
$$j = m \text{ or } n$$

$$k^{(h)}(M_S) = K^{(h)}(M_S) \cdot h / K^{(h)}(M_S)$$

$$|A_1^{(j)}|^2 = (\tilde{k}^{(j)} \cdot A^{(j)} \cdot \tilde{A}^{(j)} \cdot k^{(j)}) - (K^{(j)})^2$$

$$A_2^{(j)} = \det A^{(j)}/K^{(j)}$$

$$A_3^{(j)} = \operatorname{Tr} \tilde{A}^{(j)} \cdot A^{(j)} - (\tilde{k}^{(j)} \cdot A^{(j)} \cdot \tilde{A}^{(j)} \cdot k^{(j)})$$

$$|Q_1^{(j)}|^2 = (\tilde{k}^{(j)} \cdot (Q^{(j)})^2 \cdot k^{(j)}) - (\tilde{k}^{(j)} \cdot Q^{(j)} \cdot k^{(j)})^2$$
$$j = m \text{ or } n$$

$$|Q_2^{(j)}|^2 = 2 \operatorname{Tr} (Q^{(j)})^2 - 4(\tilde{k}^{(j)} \cdot (Q^{(j)})^2 \cdot k^{(j)}) + (\tilde{k}^{(j)} \cdot Q^{(j)} \cdot k^{(j)})^2$$
$$j = m \text{ or } n$$

$$g^2 K^{(m)} K^{(n)} L^{(M,N)} = \tilde{h} \cdot \tilde{g} \cdot (\tilde{A}^{(m)} \cdot A \cdot \tilde{A}^{(n)} \cdot A^{(n)} + \tilde{A}^{(n)} \cdot A^{(n)} \cdot \tilde{A}^{(m)} \cdot A^{(m)}) \cdot g \cdot h$$

$$g K^{(m)} K^{(h)}(M_S) P^{(m,h)} = \tilde{h} \cdot \tilde{g} \cdot (\tilde{A}^{(m)} \cdot A^{(m)} \cdot \tilde{g}^{-1} \cdot \tilde{K}^{(h)}(M_S) \cdot A^{(h)} + \tilde{g}^{-1} \cdot \tilde{K}^{(h)}(M_S) \cdot A^{(h)} \cdot \tilde{A}^{(m)} \cdot A^{(m)}) \cdot g \cdot h - 2(K^{(m)})^2(\tilde{h} \cdot \tilde{K}^{(h)}(M_S) \cdot A^{(h)} \cdot g \cdot h)$$

Hence, to second order, ENDOR signal frequencies for nitrogen nuclei are expressed as

$$h\nu_{ENDOR}(M_S, M_I^{(n)} \leftrightarrow M_I^{(n)} - 1) = K^{(n)} M_S + \tfrac{3}{2}(\tilde{k}^{(n)} \cdot Q^{(n)} \cdot k^{(n)})(2M_I^{(n)} - 1) - g_N \beta_n H(k^{(n)} \cdot h) + \frac{1}{2g\beta H}[|A_1^{(n)}|^2 M_S(2M_I^{(n)} - 1) - \tfrac{1}{2}A_2^{(n)} - \tfrac{1}{2}A_3^{(n)} M_S(2M_I^{(n)} - 1) + (L^{(m,n)} - 2K^{(m)}K^{(n)})M_S M_I^{(m)}] + \frac{1}{2K^{(n)} M_S}[|Q_1^{(n)}|^2(24(M_I^{(n)})^2 - 24M_I^{(n)} + 1) - \tfrac{1}{4}|Q_2^{(n)}|^2(6(M_I^{(n)})^2 - 6M_I^{(n)} - 1)] \quad (A5)$$

and for protons

$$h\nu_{ENDOR}(M_S) = K^{(h)}(M_S) - \frac{\det A}{4g\beta H K^{(h)}(M_S)}[M_S - g_H \beta_n H(\tilde{h} \cdot \tilde{g} \cdot (A^{(h)})^{-1} \cdot h)/g] + \frac{1}{2g\beta H}P^{(m,h)} M_S M_I^{(m)} \quad (A6)$$

Registry No. Cu(salen), 34754-33-1; Ni(salen), 14167-20-5.

References and Notes

(1) (a) G. H. Rist and J. S. Hyde, *J. Chem. Phys.*, **50**, 4532 (1969); (b) *ibid.*, **52**, 4633 (1970); (c) R. Böttcher, D. Heinhold, and W. Windsch, *Chem. Phys. Lett.*, **49**, 148 (1977); (d) T. G. Brown, J. L. Petersen, G. P. Lozos, J. R. Anderson, and B. M. Hoffman, *Inorg. Chem.*, **16**, 1563 (1977); (e) A. Schweiger, G. Rist, and Hs. H. Günthard, *Chem. Phys. Lett.*, **31**, 48 (1975); (f) A. Schweiger and Hs. H. Günthard, *Chem. Phys.*, **32**, 35 (1978).
(2) A. H. Maki and B. R. McGarvey, *J. Chem. Phys.*, **29**, 35 (1958); (b) B. W. Moores and R. L. Belford, "Electron Spin Resonance of Metal Complexes", Teh Fu Yen, Ed., Plenum Press, New York, 1969, p 13; (c) M. I. Scullane and H. C. Allen, Jr., *J. Coord. Chem.*, **4**, 255 (1975); (d) V. Malatesta and B. R. McGarvey, *Can. J. Chem.*, **53**, 3791 (1975).
(3) P. Pfeiffer, B. Breith, E. Lubbe, and T. Tsumaki, *Justus Liebigs Ann. Chem.*, **84**, 503 (1933).
(4) L. M. Shkol'nikova, E. M. Yumal, E. A. Shugam, and V. A. Voblikova, *Zh. Strukt. Khim.*, **11**, 886 (1970).
(5) M. Iwasaki, *J. Magn. Reson.*, **16**, 417 (1974).
(6) The quadrupole coupling data for ^{63}Cu were obtained from ^{63}Cu ENDOR of Cu(salen). Details of the measurement and analysis of the copper ENDOR will be reported elsewhere.
(7) J. R. Morton, *Chem. Rev.*, **64**, 453 (1964).
(8) (a) P. L. Orioli, E. C. Lingafelter, and B. W. Brown, *Acta Crystallogr.*, **17**, 1113 (1964); (b) D. Hall and T. N. Waters, *J. Chem. Soc.*, 2644 (1960).
(9) Details of the calculation will be reported elsewhere.
(10) Y. H. Hsieh, P. S. Ireland, and T. L. Brown, *J. Magn. Reson.*, **21**, 445 (1976).
(11) J. A. Weil, *J. Magn. Reson.*, **18**, 113 (1975).
(12) A. Schweiger, F. Graf, G. Rist, and H. H. Günthard, *Chem. Phys.*, **17**, 155 (1976).